Piotr GAS, Paweł SCHMIDT

AGH University of Science and Technology

Impact of tissue parameters on temperature distribution in time-transient analysis of interstitial microwave hyperthermia

Abstract. *This article relates to the application of the coaxial-slot antenna in pathological tissue treatment during interstitial microwave hyperthermia. Electromagnetic field radiated from the antenna in TM wave form is the source of the temperature gradient in the tissue. Therefore, besides the wave equation, the Pennes equation under transient condition is examined. The influence of the parameters of various tissues on temperature distribution is investigated. All simulation results have been calculated using the FEM for the antenna operating frequency of 2.45 GHz and the antenna input power level set to 1W.*

Streszczenie. *Artykuł odnosi się do zastosowania anteny współosiowej ze szczeliną powietrzną w leczeniu patologicznych tkanek podczas śródmiąższowej hipertermii mikrofalowej. Pole elektromagnetyczne wytwarzane przez antenę w postaci fali TM stanowi źródło gradientu temperatury w tkance. Z tego względu, oprócz równania falowego rozpatrzono równanie Pennesa w przypadku niestacjonarnym. Zbadano wpływ parametrów różnych tkanek na rozkład temperatury. Wyniki symulacji zostały wyznaczone przy użyciu MES dla częstotliwości pracy anteny 2,45 GHz oraz poziomu mocy wejściowej anteny 1 W.* ***(Wpływ parametrów tkanki na rozkład temperatury w analizie czasowej śródmiąższowej hipertermii mikrofalowej)***

Keywords: interstitial microwave hyperthermia, coaxial-slot antenna, bioheat equation
Słowa kluczowe: śródmiąższowa hipertermia mikrofalowa, antena współosiowa ze szczeliną powietrzną, biologiczne równanie ciepła

Introduction

Interstitial microwave hyperthermia is a special treatment procedure in which temperature of the diseased tissues is elevated to the range of $40 - 46^{\circ}\mathrm{C}$ [1] using high frequency needle electrodes, microwave antennas, ultrasound transducers, laser fibre optic conductors, or ferromagnetic rods, seeds or fluids located deep within the human body [2]. Invasive hyperthermia systems equipped with elements mentioned above have several technical advantages over non-invasive ones. First of all, they provide heat directly into the tumor or malignant tissues while minimally affecting the surrounding healthy [1]. This causes the induction of thermonecrosis of the tissues at the distance of 1 to 2 cm around the heat source [3]. Moreover, they offer the possibility of better controlling the temperature increments and distribution inside both normal and cancerous tissue. It is an immensely important issue because when the temperature exceeds $46^{\circ}\mathrm{C}$ ablative heating occurs and all tissues are destroyed.

As interstitial applicators typical monopole antenna made from coaxial cable with alternating layers of conductor and dielectric are frequently used [2]. They may contain an air gap which causes the temperature gradient to take the largest value in its immediate vicinity as shown in the presented simulation. Medical practice has shown that this technique is suitable for the treatment of brain, liver, breast, kidney, bone and lung tumors [4] whose diameter does not exceed 5 cm [3]. What's more, interstitial microwave hyperthermia has been successfully used as an adjuvant treatment in other cancer therapies such as radiotherapy or chemotherapy as well as immunotherapy or gene therapy [1]. Total treatment time, depending on the tumor type and degree of its progress can vary from 30 to 60 minutes.

In recent years an increasing number of scientific research is focused on the topic of hyperthermia which demonstrates that this aspect is still important and new solutions in hyperthermia treatment are researched [5, 6]. Moreover, the testing of the use of magnetic nanoparticles in cancer treatment and the development of the so-called nanothermy has been observed [7]. Talking about hyperthermia, one cannot ignore its historical context, as shown in [8]. Despite a long history, further investigation into hyperthermia techniques is necessary to make this method simpler, safer and widely available for patients.

Geometrical model and basic equations

A schematic view of the model of the microwave antenna is shown on Figures 1 – 2. It specifies such elements as central conductor, dielectric, outer conductor and a plastic catheter. The last one fulfils the protective purpose for the other elements of the antenna. The air slot with size d is placed in the outer conductor. The dimensions of the coaxial-slot antenna are taken from [4] and put together in Table 1. What is interesting, the antenna is thin and its width does not exceed 2 mm. Due to the axial-symmetrical model cylindrical coordinates r, ϕ, z are used. The presented 2-dimensional model includes only half of the antenna structure and the surrounding human tissue. What is important, the whole 3-dimensional model can be obtained by rotating the 2-dimentional one along the z axis.

To derive the governing equations let us start with the Maxwell's equations in the frequency domain:

$$\nabla \times \boldsymbol{H} = \boldsymbol{J} + \mathrm{j}\omega \boldsymbol{D} \tag{1}$$

$$\nabla \times \boldsymbol{E} = -\mathrm{j}\omega \boldsymbol{B} \tag{2}$$

where $\boldsymbol{E}$ and $\boldsymbol{H}$ are the electric and magnetic field strengths, respectively, $\boldsymbol{J}$ is the current density and $\boldsymbol{D}$, $\boldsymbol{B}$ are adequately the vectors of electric displacement density and magnetic induction. Moreover, j is the imaginary unit and ω is the angular frequency of the EM field.

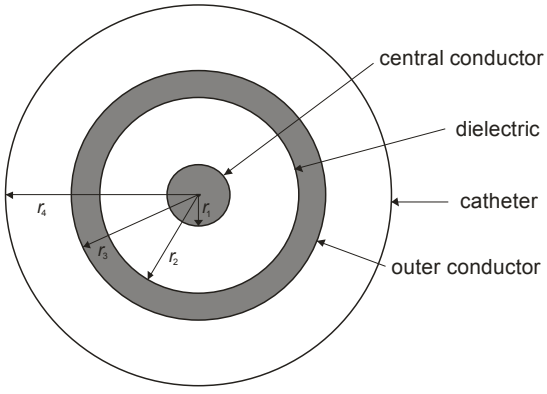

Fig.1. Cross section of the antenna with geometrical dimensions

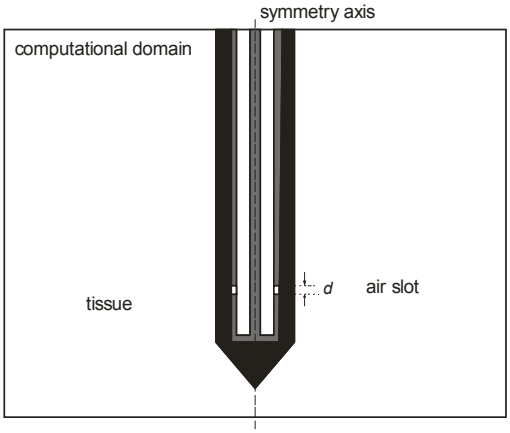

Fig.2. Model of the coaxial antenna located in the human tissue

Table 1. Dimensions of the microwave antenna (m^{-3})

radius of the central conductor	r_1 = 0.135
inner radius of the outer conductor	r_2 = 0.470
outer radius of the outer conductor	r_3 = 0.595
radius of the catheter	r_4 = 0.895
size of the air slot	d = 1

After considering the Ohm's law in the differential form $\boldsymbol{J} = \sigma \boldsymbol{E}$ and material dependencies $\boldsymbol{D} = \varepsilon_0 \varepsilon_r \boldsymbol{E}$ and $\boldsymbol{B} = \mu_0 \mu_r \boldsymbol{H}$, for uniform, linear and isotropic medium, equations (1) and (2) in the complex domain assumes the form

$$\nabla \times \boldsymbol{H} = \mathrm{j}\omega\varepsilon_0 \left(\varepsilon_r - \mathrm{j}\frac{\sigma}{\omega\varepsilon_0} \right) \boldsymbol{E} \tag{3}$$

$$\nabla \times \boldsymbol{E} = -\mathrm{j}\omega\mu_0\mu_r \boldsymbol{H} \tag{4}$$

where ε_0 and μ_0 are the permittivity and permeability of the vacuum, ε_r and μ_r are the relative permittivity and relative permeability of the medium, respectively and where σ is the electrical conductivity of the body.

Then after applying the rotation operator to both sides of equation (3) and substituting equation (4) into (3) the following wave equation can be obtained

$$\nabla \times \left[\underline{\varepsilon}_r^{-1} \nabla \times \boldsymbol{H} \right] - \mathrm{k}_0^2 \mu_r \boldsymbol{H} = 0 \tag{5}$$

In the above equation $\underline{\varepsilon}_r$ is the complex relative permittivity approximated with the Cole-Cole model [9] as follows

$$\underline{\varepsilon}_r(\omega) = \varepsilon_\infty + \frac{\varepsilon_s - \varepsilon_\infty}{1 + (j\omega\tau_0)^{1-\alpha}} - \mathrm{j}\frac{\sigma_s}{\omega\varepsilon_0} \tag{6}$$

where ε_∞ is the infinite limit of relative permittivity, ε_s – the static limit of relative permittivity, α – the Cole–Cole parameter, τ_0 – the relaxation time constant (ps) and σ_s – the static conductivity (S/m). What is more, k_0 is the free-space wave number given by the equation

$$\mathrm{k}_0 = \frac{\omega}{\mathrm{c}_0} = \omega\sqrt{\varepsilon_0\mu_0} \tag{7}$$

and c_0 is the speed of light in vacuum.

Since the analysed model is axial-symmetrical, transverse magnetic (TM) waves are used and there are no electric field variations in the ϕ -direction. A magnetic field strength has only tangential component and an electric field strength propagates in the *r-z* plane as follows

$$\boldsymbol{H} = H_\phi \boldsymbol{e}_\phi \tag{8}$$

$$\boldsymbol{E} = E_r \boldsymbol{e}_r + E_z \boldsymbol{e}_z \tag{9}$$

Considering the above, the wave equation takes the scalar form

$$\nabla \times \left[\underline{\varepsilon}_r^{-1} \nabla \times H_\phi \right] - \mathrm{k}_0^2 \mu_r H_\phi = 0 \tag{10}$$

For all metallic surfaces PEC (perfect electric conductor) boundary conditions are used as written below

$$\boldsymbol{n} \times \boldsymbol{E} = 0 \tag{11}$$

where $\boldsymbol{n}$ is the unit vector normal to the surface. Furthermore, the external boundaries of the computational domain, which do not represent a physical boundary have the so-called matched boundary conditions that make the boundaries totally non-reflecting and they assume the following equation

$$\sqrt{\varepsilon_0 \underline{\varepsilon}_r}\, \boldsymbol{n} \times \boldsymbol{E} - \sqrt{\mu} H_\phi = -2\sqrt{\mu} H_{\phi 0} \tag{12}$$

where $H_{\phi 0}$ is an input field incident on the antenna as shown bellow

$$H_{\phi 0} = \frac{1}{Z r} \sqrt{\frac{Z P_{\mathrm{in}}}{\pi \ln(r_2 / r_1)}} \tag{13}$$

Further, P_{in} is the total input power in the dielectric, r_1 and r_2 are the dielectric's inner and outer radii, respectively, while Z signifies the wave impedance of the dielectric, which is determined by

$$Z = \frac{\mathrm{Z}_0}{\sqrt{\varepsilon_r}} \approx \frac{377}{\sqrt{\varepsilon_r}} \tag{14}$$

where Z_0 is the wave impedance in vacuum.

Moreover, on the symmetry axis of the antenna it is established as follows

$$E_r = 0 \quad , \quad \frac{\partial E_z}{\partial r} = 0 \tag{15}$$

What is important, the seed point is modelled using a port boundary condition with the power level set to P_{in} = 1W at the low-reflection external boundary of the dielectric cable. The full derivation of equation (10) can be found in [10].

The wave equation is conjugated with temperature field using the Pennes equation formulated in the mid-twentieth century [11]. The so-called bioheat equation describes the phenomenon of heat transfer in biological tissues and in transient analysis it is expressed by

$$\rho C \frac{\partial T}{\partial t} + \nabla\left(-k\nabla T\right) = \rho_\mathrm{b} C_\mathrm{b} \omega_\mathrm{b} (T_\mathrm{b} - T) + Q_{\mathrm{ext}} + Q_{\mathrm{met}} \tag{16}$$

where T is the body temperature (K), k – the tissue thermal conductivity (W m^{-2} K^{-1}), ρ – the tissue density (kg m^{-3}), C – the tissue specific heat (J kg^{-1} K^{-1}), T_b – the blood vessel temperature (K), ρ_b – the blood density (kg m^{-3}), C_b – the blood specific heat (J kg^{-1} K^{-1}), ω_b – the blood perfusion rate (s^{-1}) and t – the time (s).

What is more interesting, the described model takes into account the so-called the metabolic heat generation Q_{met} (W m^{-3}) as well as the external heat sources Q_{ext} (W m^{-3}), which are relevant to volumetric power densities. The last one is responsible for the changing of the temperature inside the human tissue as

$$Q_{\text{ext}} = \frac{1}{2}\sigma\, \boldsymbol{E}\cdot\boldsymbol{E}^{*} = \frac{1}{2}\sigma\left|\boldsymbol{E}\right|^{2} \tag{17}$$

The Pennes equation (16) requires the specifications of both the initial and boundary conditions to be solved. The initial one is given by

$$T = T_0 = 37°\text{C} \tag{18}$$

which corresponds to the physiological temperature of the human brain. The computational domain is limited to a part of the human tissue, that is why it can be assumed that the heat exchange between parts of the same tissue does not take place and the boundary condition describing this process uses thermal insulation as follows

$$\boldsymbol{n}\cdot\left(k\nabla T\right) = 0 \tag{19}$$

Computational results

The presented simulation assumes that the human tissue and antenna are considered as uniform mediums with constant material parameters. The antenna operates at the frequency of 2.45 GHz and the antenna input power level is set to 1W. Electrical parameters of the microwave antenna are given in Table 2. The blood parameters are summarized in Table 3. Other tissue parameters for the adopted working frequency of antenna are put together in Table 4. What is worth noting, the metabolic heat generation of the tissue is omitted because usually $Q_{\text{met}} << Q_{\text{ext}}$. Moreover, main equations (10) and (16) with the appropriate boundary conditions were solved using the finite element method.

Table 2. Electrical parameters of the coaxial-slot antenna [4]

	Re[$\underline{\varepsilon}_{\text{r}}$]	μ_{r}	σ (S m^{-1})
dielectric	2.03	1	0
catheter	2.60	1	0
air slot	1	1	1

Table 3. Physical parameters of blood taken in the model [12]

Tissue	ρ_{b} (kg m^{-3})	C_{b} (J kg^{-1}·K^{-1})	T_{b} (K)	ω_{b} (s^{-1})
blood	1020	3640	310.15	0.004

All calculated results are summarized in Figures 3 – 6. Fig. 3 shows the distribution of equipotential lines in the lung tissue for modulus of the magnetic field strength and temperature at three various moments of time. Next illustrations demonstrate the temperature distributions for different tissues along the two paths that pass through the human tissue perpendicular to the antenna at the height of the air slot (Fig. 4) and parallel to the symmetry axis of the antenna at the distance of 2.5 mm (Fig. 5). Time dependent temperature distributions for several various distances from the microwave antenna are shown in Fig. 6.

Table 4. Physical parameters of various human tissues [12, 13]

Tissue	ε_{∞}	ε_{s}	τ_0 (ps)	α	σ_{s} (S/m)
brain	4.0	32	7.958	0.1	0.02
kidney	4.0	47	7.958	0.1	0.05
lung	2.5	18	7.958	0.1	0.03
breast	2.5	3	17.680	0.1	0.01
liver	4.0	39	8.842	0.1	0.02

Tissue	k (W m^{-1}·K^{-1})	ρ (kg m^{-3})	C (J kg^{-1}·K^{-1})
brain	0.51	1046	3630
kidney	0.53	1066	3763
lung	0.39	394	3886
breast	0.33	1058	2960
liver	0.52	1079	3540

Summary

In this paper the influence of various tissue parameters on temperature distribution has been investigated. Since interstitial microwave hyperthermia gains new fields of application in the treatment of liver, breast, kidney, brain and lung tumors that is why these types of tissues were used in the presented simulations. It should be noted that tissue parameters such as permittivity as well as electric and thermal conductivity cannot be arbitrarily changed because they are closely connected with the frequency and type of human tissue. As predicted, the temperature inside the tissue become smaller with the distance from the microwave antenna and its largest values are focused near the antenna's air gap. Initially, the greatest and the lowest temperatures are reached in lung and liver, respectively. Over time, the highest temperature values are observed in breast tissue. Furthermore, the smallest temperature changes occur in the lung because its temperature quickly reaches a steady state compared to other tissues (after a period of only 400 s). What is interesting, very close temperatures occur in the kidney and brain tissues forasmuch they are similar in properties. Moreover, the values of tissue temperature can be easily changed by adjusting the total input power of the antenna.

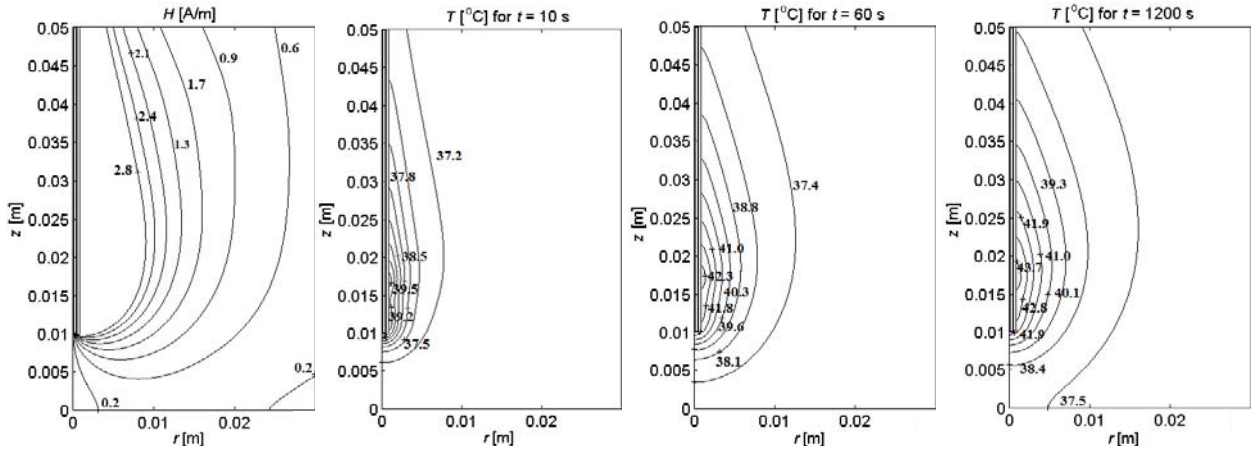

Fig.3. Equipotential lines of the module of the magnetic field strength and temperature distributions for different moments of time 10 s, 60 s and 1200 s (steady-state) respectively in order from left to right (all for the lung tissue, f = 2.45 GHz and P_{in} = 1W)

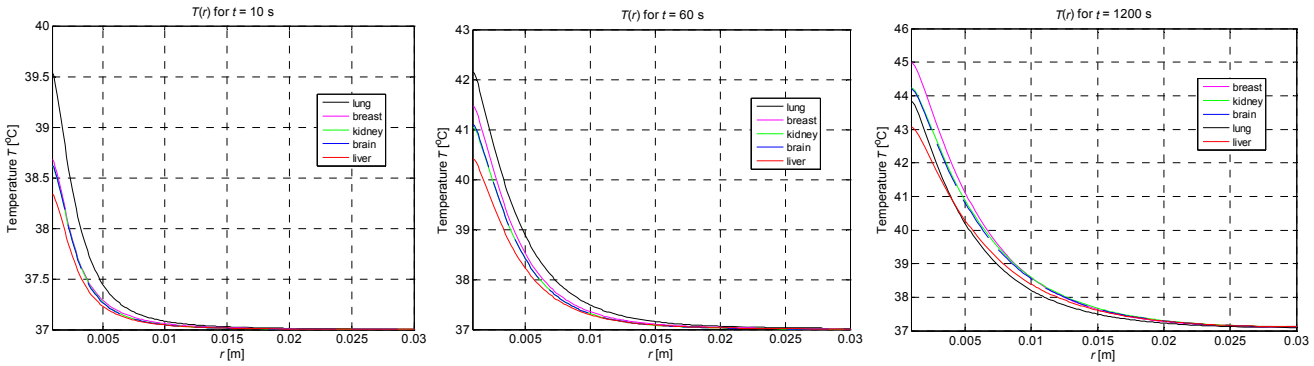

Fig.4. Temperature distributions for various tissues along the path $z = 16$ mm for different moments of time ($f = 2.45$ GHz and $P_{in} = 1$W)

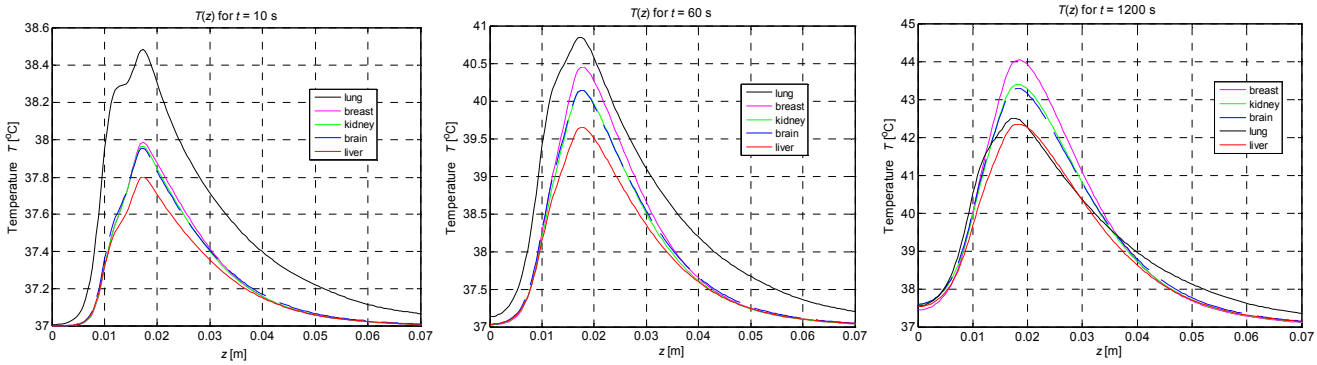

Fig.5. Temperature distributions for various tissues along the path $r = 2.5$ mm for different moments of time ($f = 2.45$ GHz and $P_{in} = 1$W)

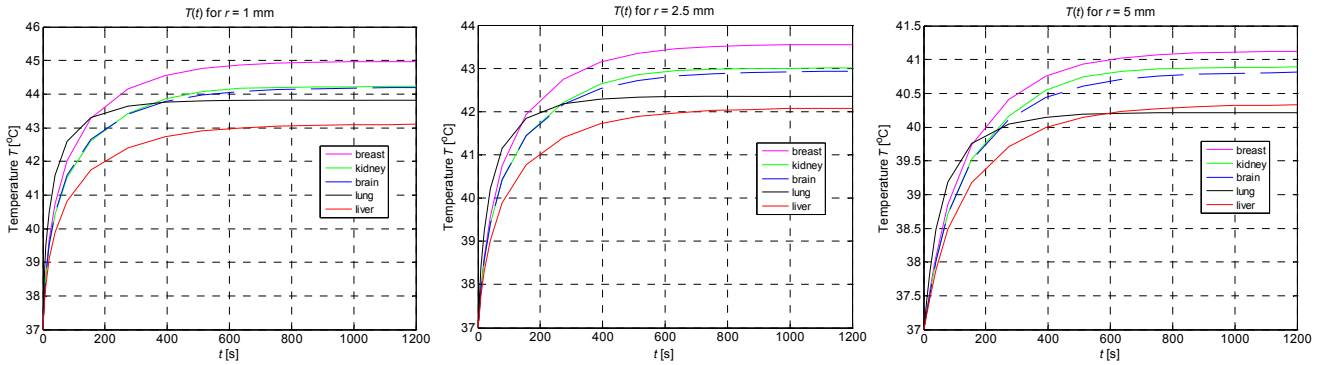

Fig.6. Transient temperature distributions for various tissues at the points lying along the path $z = 16$ mm for different distances from the antenna: $r = 1$ mm, $r = 2.5$ mm and $r = 5$ mm respectively in order from left to right ($f = 2.45$ GHz and $P_{in} = 1$W)

REFERENCES

[1] McPhee S.J., Papadakis M.A., Rabow M.W., *Current Medical Diagnosis and Treatment 2013*, 52nd edition, McGraw-Hill Medical (2012).

[2] Balanis C.A., *Modern Antenna Handbook*, John Wiley & Sons (2008).

[3] Baronzio G.F., Hager E.D., *Hyperthermia in Cancer Treatment: A Primer*, Landes Bioscience and Springer Science + Business Media, New York (2006).

[4] Saito K., Hosaka S., Okabe S.Y., A proposition on improvement of a heating pattern of an antenna for microwave coagulation therapy: introduction of a coaxial-dipole antenna, *Electronics and Communications in Japan (Part I: Communications)*, 86 (2003), No. 1, 16-23.

[5] Gas P., Temperature inside Tumor as Time Function in RF Hyperthermia, *Electrical Review*, 86 (2010), No. 12, 42-45.

[6] Kurgan E., Gas P., Treatment of Tumors Located in the Human Thigh using RF Hyperthermia, Electrical Review, 87 (2011), No. 12b, 103-106.

[7] Barglik J., Dołęga D., Nanotermia oraz przykłady zastosowania pól elektromagnetycznych w medycynie, *Przeglad Elektrotechniczny*, 86 (2010), No. 7, 15-19.

[8] Gas P., Essential Facts on the History of Hyperthermia and their Connections with Electromedicine, *Electrical Review*, 87 (2011), No. 12b, 37-40.

[9] Cole K.S., Cole R.H., Dispersion and absorption in dielectrics I: Alternating Current. Characteristics, *J. Chem. Phys.*, 9(1941), 341-351.

[10] Gas P., Temperature Distribution of Human Tissue in Interstitial Microwave Hyperthermia, *Electrical Review*, Vol. 88 (2012), No. 7a, 144-146.

[11] Pennes H.H., Analysis of Tissue and Arterial Blood Temperatures in the Resting Human Forearm, *J. Appl. Physiol.*, 1 (1998), No. 85, 5-34.

[12] Mcintosh R. L., Anderson V., A Comprehensive Tissue Properties Database Provided for the Thermal Assessment of a Human at Rest, *Biophysical Reviews and Letters*, 5 (2010), No. 3, 129-151.

[13] Gabriel S., Lau R.W., Gabriel C., The dielectric properties of biological tissues: II. Measurements in the frequency range 10 Hz to 20 GHz, *Phys. Med. Biol.*, 41 (1996), 2251-2269.

***Authors**: mgr inż. Piotr Gas, dr inż. Paweł Schmidt, AGH University of Science and Technology, Department of Electrical and Power Engineering, al. Mickiewicza 30, 30-059 Krakow, E-mail: piotr.gas@agh.edu.pl , pschmidt@agh.edu.pl*